Mössbauer and energy-dispersive x-ray-diffraction studies of the pressure-induced crystallographic phase transition in C-type Yb_2O_3

C. Meyer,* J. P. Sanchez, and J. Thomasson
Commissariat à l'Energie Atomique, Département de Recherche Fondamentale sur la Matière Condensée, 38054 Grenoble Cedex 9, France

J. P. Itié
Physique des Milieux Condensés, Université Pierre et Marie Curie, 4 Place Jussieu, BP 77, 75252 Paris Cedex 5, France and Laboratoire pour l'Utilisation du Rayonnement Electromagnétique, Université Paris-Sud, Bâtiment 209D, 91405 Orsay, France
(Received 31 October 1994; revised manuscript received 17 January 1995)

The high-pressure behavior of the cubic C-type Yb_2O_3 was investigated by ^{170}Yb Mössbauer spectroscopy and energy-dispersive x-ray diffraction. The room-temperature x-ray-diffraction data show that C-Yb_2O_3 transforms to the monoclinic B-type structure above 13 GPa. The equation of state of both C- and B-type phases was derived from these experiments. Mössbauer measurements up to 20 GPa were carried out at 4.2 K using a Merrill-Bassett-type anvil cell. They confirm the occurrence of a pressure-induced phase transition. The pressure (volume) dependence of the lattice and $4f$ contributions to the electric-field gradient at the Yb^{3+} ions in the C phase is discussed.

I. INTRODUCTION

Since the introduction of diamond anvil cells (DAC), Mössbauer spectroscopy has been proved to be a powerful technique for high-pressure studies. Various problems have taken advantage of its great efficiency: structural transformation,[1] metal-insulator transition,[2] enhancement or collapse of magnetic ordering,[1-3] amorphization,[4] etc. Recently Sterer, Pasternak, and Taylor[5] described a miniature cell well suited for low-temperature measurements in a standard Mössbauer cryostat. This Merrill-Bassett-type DAC shows very good performances for its small size ($\phi \approx 22$ mm), as it can reach 50 GPa, when using reduced diamond culets. These authors have achieved successful experiments for several Mössbauer isotopes ^{119}Sn, ^{57}Fe, ^{129}I, ^{151}Eu.[6] The aim of the present work was to make use of this facility for the ^{170}Yb isotope, ytterbium being one of the anomalous rare-earth elements for which numerous of interesting experiments may involve very high pressures.

Some high-pressure measurements with ytterbium have been already performed using B_4C anvil cells, up to 15 GPa.[7,8] In the present work we wanted to obtain more than 20 GPa, checking the results with a simple known compound Yb_2O_3, which belongs to the rare-earth sesquioxide series of recent interest for high-pressure structural studies,[9-11] as well as for quadrupole hyperfine interaction investigations.[12-15] A parallel structural study under pressure on a synchrotron radiation diffraction setup was carried out to determine the equation of state for this oxide, in order to compare the pressure variation of the hyperfine data with volume contraction.

II. STRUCTURAL DATA

Yb_2O_3 belongs to the rare-earth sesquioxides R_2O_3 series which is known to exhibit polymorphous crystallographic structures.[16] Three phases have been observed below 2000 °C: Cubic (bcc) denoted as C, space group $Ia\bar{3}$ (no. 206) with 16 formula per unit cell; monoclinic denoted as B, space group $C2/m$ (no. 12) with 6 formula per unit cell; hexagonal denoted as A, space group $P\bar{3}m1$ (no. 164) with 1 formula per unit cell. A to B and C to B transformations are reversible at high temperature. For each oxide only one form is stable: A-type for light rare-earths elements; B-type for Sm to Gd; and C-type for the heavy rare-earth elements. Increasing temperature above 2000 °C is not sufficient for the heaviest rare-earth elements to reach the B structure.

As a matter of fact, the R_2O_3 monoclinic phases have been obtained from cubic phases by Hoekstra[17] when applying pressure between 1 and 5 GPa at temperatures ranging from 550 °C to 1450 °C. For Yb_2O_3, conditions were, e.g., 1000 °C and 3 GPa. The B phase is metastable: when heating at 1000 °C, the C phase is recovered. Considering the thermal phase diagram versus ionic rare-earth radius (see also Fig. 28.2 of Ref. 16), Hoekstra showed that increasing pressure would create a whole displacement towards the lower radii, that is, a lowering of the transition temperatures between B and C phases.

The B phase can also be obtained using a vapor quenching method described by Coutures *et al.*[18] The lattice parameters for Yb_2O_3 (B) obtained by the two methods are $a = 13.73(1)$ Å, $b = 3.425(3)$ Å, $c = 8.452(8)$ Å, and $\beta = 100.17(5)°$ (Ref. 17); and $a = 13.72$ Å, $b = 3.428$ Å, $c = 8.437$ Å, and $\beta = 100.18°$ (Ref. 18).

Notice that similar phase transitions under shock wave compression have been found in rare-earth sesquioxides, which show C-type → A-type transition and A-type → B-type reverse transition during shock loading and unloading, respectively.[9] On the other hand, in contrast to our results, Fujimura *et al.* reported that under static condition at room temperature, C-Yb_2O_3 transforms to a high-pressure phase with A-type structure at 15 GPa.[10]

It is interesting to compare the volume per formula unit for the C and B phases. Taking $a=10.4342(4)$ Å for the cubic structure,[19] we obtain $V_C=42.74$ cm^3/mol to be compared to $V_B=39.25$ cm^3/mol for the monoclinic structure which represents a volume contraction of 8%.

We show in the present paper that applying very high pressure induces C to B transformation at room temperature. The comparison with structural data may check the performances of our ^{170}Yb Mössbauer high-pressure experiment.

III. LOCAL SYMMETRY FOR YTTERBIUM

In the cubic phase the Yb ions occupy two octahedral sites, 1/4 in 8a positions with a three-fold inversion symmetry C_{3i}, and 3/4 in 24d positions with a two-fold symmetry C_2. These two sites can be viewed as the center of an oxygen cube: for the C_{3i} site two oxygen atoms are missing across the body diagonal while for the C_2 site they are missing across a face diagonal.

On the other hand in the monoclinic structure, the Yb ions occupy three equally populated sites, sitting all in 4i positions with a mirror plane. Two of them are seven coordinated, with the seventh oxygen atom pointing along [111] directions out of the faces of a trigonal prism, while one site is octahedral. The relationship between the C and B structures is not simple because the ytterbium atoms are displaced with respect to the oxygen basic array going from the cubic to monoclinic phase. The C-type to B-type transformation is classified as a reconstructive transition (i.e., there is extensive breaking of bonds).[20]

Concerning the hyperfine interactions measured by Mössbauer spectroscopy, it is anticipated that they must be very sensitive to any structural change because the five sites involved have rather different local symmetries.

IV. EXPERIMENT

Mössbauer spectroscopy

The small size of the DAC described by Sterer *et al.*[5] for Mössbauer spectroscopy, is well suited for low-temperature experiments required by the 84.3-keV transition energy of ^{170}Yb. However the main problem for a high-energy Mössbauer transition is the collimation of the γ rays which cannot be achieved through the gasket itself, even made of heavy element alloys such as $Ta_{0.9}W_{0.1}$. For example a 50-μm-thick gasket, which corresponds to usual requirement for pressure above 10 GPa, only absorbs 50% of the ^{170}Yb γ rays. As a consequence, an external Ta collimator has been added and placed as close as possible to the entrance diamond. A thickness of 0.5 mm is enough to stop 99.9% of the photons. In this way we were able to increase by a factor of 2 the absorption area of the Mössbauer spectrum. The small volume ($\approx 10^{-6}$ cm^3) available inside the pressure chamber could be a serious problem for ^{170}Yb which is only 3% abundant in natural ytterbium. However, for a 50-μm-thick gasket and a 300-μm hole, an isotopic enrichment of 50% may be generally good enough for any Yb compound. Either argon or a methanol-ethanol mixture were used as a pressure medium. Pressures were measured at 77 K with the ruby-fluorescence method. Uncertainties in pressures did not exceed 0.3 GPa.

A small size ^{170}Tm $^{11}B_{12}$ source[21] has been worked out in order to improve the source-absorber diameter ratio. A TmB_{12} chip of 2-mm diam has been irradiated in a 10^{14} n/cm^2 s neutron flux during five days resulting in an activity of about 35 mCi. In order to get rid of the subsequent defects, an annealing at 1100 °C during 5 h has been performed. Two such sources have been successively prepared. The small grain was then embedded in a source holder which is allowed to run at less than 2 mm from the cell. Both source and absorber were cooled down to helium temperature. The quality of the sources was checked using a single line YbB_6 absorber. The experimental linewidth Γ was found to be typically 3.25(5) mm/s to be compared with the natural linewidth of 2.02 mm/s. This significative broadening can be explained by the high specific activity giving rise to defects difficult to eliminate even with the annealing process. Natural Yb absorbers containing 300 mg Yb/cm^2 were taken for standard measurements. For high-pressure experiments 70% enriched ytterbium oxide was used. The 84.3-keV γ rays were counted with an intrinsic Ge detector and typical count rates through the DAC were about 2000 counts per second.

Synchrotron radiation energy-dispersive x-ray-diffraction (EDXRD)

The diffraction experiments were carried out on the EDX station for high pressure at LURE. It is located on the DCI wiggler beamline DW11. The energy range available is 10–50 keV. The orientation of the germanium detector is possible in the 2θ range of $-5°$ to $+25°$. The DAC has been described elsewhere.[22] The pressure increase is monitored by applying helium gas pressure on a membrane which compresses the diamonds. Silicon oil was used as an hydrostatic medium. The dimensions of the pressure chamber are 200 μm$\times$50 μm. The pressure was measured with the shifts of the fluorescence lines of ruby chips introduced in the chamber. The laser equipment is running in the reflection geometry. Experiments were performed up to 25 GPa. The error on the pressure reading is less than 0.1 GPa. In most cases it is typically 0.05 GPa. The large energy domain covered allows the analysis of good quality peaks from 15 keV up to 40 keV corresponding to interplanar distances in the range 4–1.5 Å, for a chosen θ value of about 6°. On the other hand, the Yb fluorescence lines ($K\alpha$ at about 52 keV and $K\beta$ at about 60 keV) are not troublesome in the diagram. A standard counting time is 10 mn. The analysis of the diagrams is performed with a program, fitting the positions E_{hkl} (keV) of the peaks with Gaussian line shapes. The error on the calculated positions is 5×10^{-4} to 10^{-3} keV corresponding to 10^{-5} Å in d_{hkl}.

V. RESULTS

Mössbauer experiment data

Ytterbium sesquioxide orders antiferromagnetically at 2.3 K.[23,24] Therefore only a quadrupole split spectrum is expected for each of the two Yb sites present in the cubic structure at 4.2 K. The reference 4.2 K zero-pressure Mössbauer spectrum has been measured on a standard natural Yb_2O_3 absorber (out of the HP cell) and is represented in Fig. 1(a). The counting time was 5 days. Table I(a) displays the values of the hyperfine parameters $\Delta = eQV_{zz}$ and η derived from a fit assuming two subspectra in the 3:1 intensity ratio and same linewidths. In addition, for the less populated site of C_{3i} point symmetry, a zero asymmetry parameter η is assumed. These values are in agreement with those reported in the literature.[25,26]

Figure 2 displays the Mössbauer spectra obtained between 4.2 and 20.5 GPa at 4.2 K. The spectra were collected during 11 days for most of them. At 4.2 and 12 GPa the spectra are basically the same as for zero pressure and a fit in the same conditions is satisfactory [Table I(a)]. At 13.6 GPa, however, some broadening appears, but at 16.8 and 20.5 GPa a completely different spectral shape is observed. No good fit is obtained with the above assumptions. This shape is conserved after releasing the pressure as represented in Fig. 1(b), showing large differences with the previous zero-pressure data, Fig. 1(a). This nonreversible change is attributed to a crystallographic phase transition from C to B structure as confirmed by x-ray-diffraction study (see below). In this framework a fit with three equally populated sites should hold. This was successfully done and the results are reported in Table I(b). Note that the strong broadening of the lines at 13.6 GPa may be attributed to coexistence of the two phases.

Energy-dispersive x-ray-diffraction data

Figure 3 shows three of the EDXR diagrams for 0, 12, and 18.5 GPa. Up to 13.8 GPa the peaks can be indexed in the cubic lattice. At 13.8 GPa an outer line starts to appear in the vicinity of the (321) peak while at 15.5 GPa the diagram is completely altered. The new phase can be indexed with the monoclinic structure denoted as B. After releasing the pressure, the compound is maintained in its high-pressure phase. The pressure variation of the lattice spacings is shown in Fig. 4. The transition pressure is tentatively positioned at $P = 13 \pm 1$ GPa. The full width at half maximum (FWHM) of the peaks is typically 0.6 keV. When increasing pressure a significant broadening of the peaks is observed reaching 1 keV around 15 GPa. However, this does not affect the resolution.

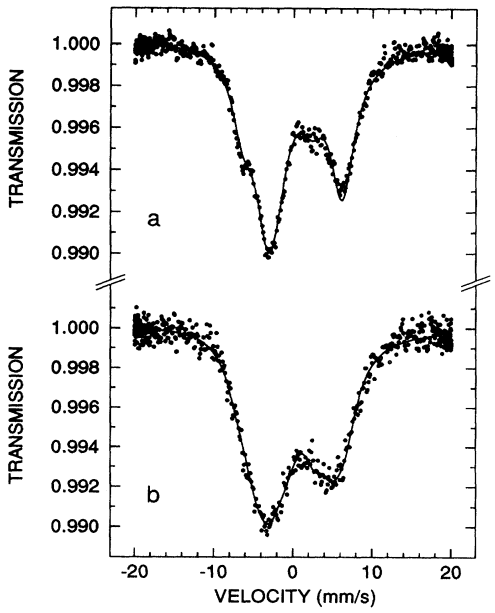

FIG. 1. Zero-pressure ^{170}Yb Mössbauer spectra at 4.2 K for Yb_2O_3: comparison between the spectra (a) before (C-type) and (b) after (B-type) applying 20 GPa.

TABLE I. ^{170}Yb Mössbauer hyperfine parameters at 4.2 K for Yb_2O_3 as a function of pressure (a) cubic structure and (b) monoclinic structure. $V/V_0(P)$ is calculated using the analytical expression derived from the Murnaghan law (see text). All values are referred to the cubic unit cell volume $V_0 = 1136$ Å^3. *, after pressure release.

(a)

		C_{3i} site (8b)	C_2 site (24d)		
P (GPa)	V/V_0	Δ (mm/s)	Δ (mm/s)	η	Γ (mm/s)
0	1	11.1(3)	25.1(1)	0.10(4)	3.71(5)
4.2	0.977(2)	11.0(4)	23.8(2)	0.25(3)	4.02(7)
12	0.945(2)	10.2(6)	23.0(2)	0.29(5)	4.26(9)
13.6	0.940(2)	10.0(8)	23.0(2)	0.39(5)	4.6(1)

(b)

		site (4i) I		site (4i) II		site (4i) III		
P (GPa)	V/V_0	Δ (mm/s)	η	Δ (mm/s)	η	Δ (mm/s)	η	Γ (mm/s)
16.8	0.841(2)	9.5(4)	0.8(2)	19.7(4)	0.73(9)	26.8(4)	0.1(1)	3.5(1)
20.5	0.826(2)	9.0(4)	1.00(4)	19.1(3)	0.59(9)	26.4(4)	0.37(8)	3.6(1)
0*	0.918(3)	12.5(4)	1.00(3)	20.8(3)	0.6(1)	27.3(4)	0.38(9)	3.7(1)

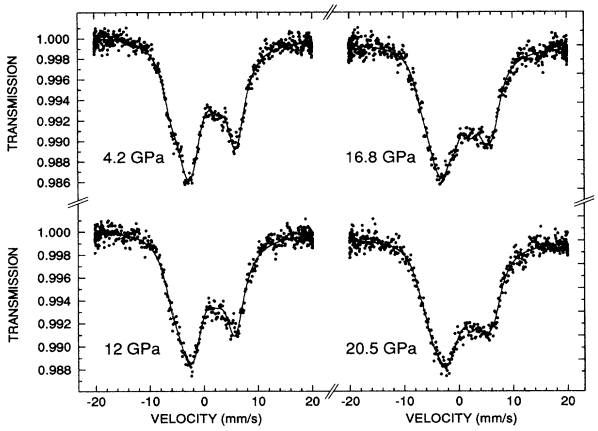

FIG. 2. Pressure dependence of the ^{170}Yb Mössbauer spectra for Yb_2O_3 at 4.2 K.

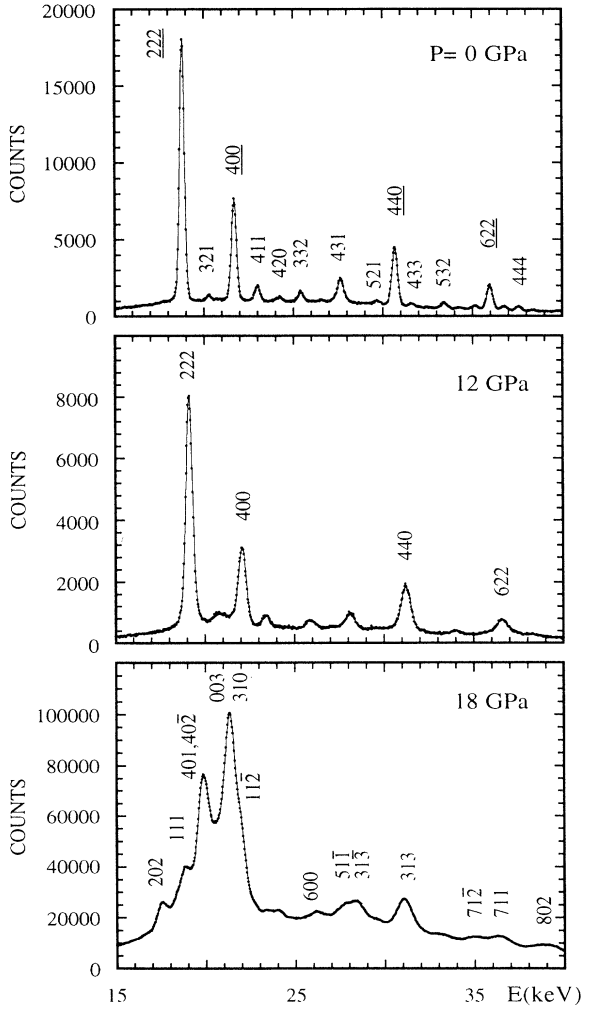

FIG. 3. Pressure dependence of the x-ray diagrams for Yb_2O_3 at room temperature.

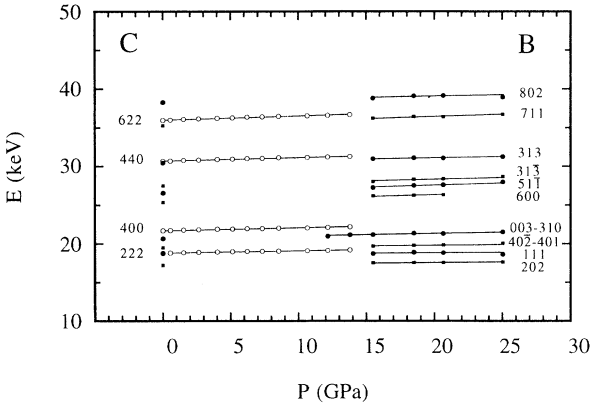

FIG. 4. Lattice spacings (hkl) as a function of pressure showing the transition from cubic C to monoclinic B structure between 12 and 14 GPa.

In the case of a cubic lattice the determination of the equation of state V/V_0 vs P does not require the knowledge of the exact value of the diffraction angle θ. What is used are the ratios $(E_0/E)^3$ for different (hkl) reflections, E_0 being the position of the peak at zero pressure. However, for the monoclinic lattice, four parameters are involved and it is not possible to relate the volume ratios easily to energy ones. Independent values of a, b, c, and β have to be derived from the EDXR diagram. The diffraction angle θ is then calculated from the zero-pressure data, taking $a=10.4342$ Å for the lattice parameter of the C phase. We obtain $\theta=6.292(2)°$.

In the cubic phase, volume compression was investigated selecting four of the most intense peaks, namely the (hkl) reflections (222), (400), (440), and (622). This allowed us to evaluate the V/V_0 value as a function of pressure, relative to the zero-pressure diagram according to $V/V_0=(E_0/E)^3$, where $V_0=1136$ Å^3 is the cubic lattice volume and refers to 16 molecules per unit cell (Fig. 5). The data have been fitted to the Murnaghan equation of state:

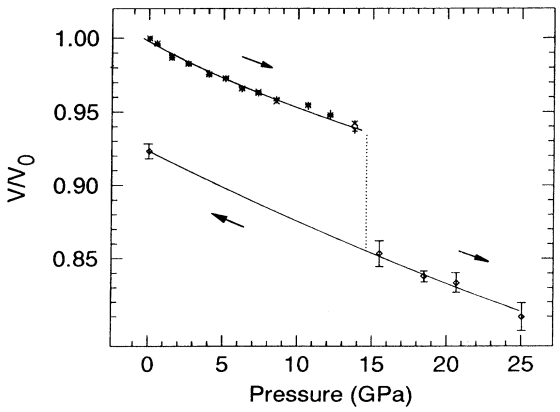

FIG. 5. Pressure variation of the lattice volume contraction referred to the cubic phase of Yb_2O_3 at room temperature and atmospheric pressure. Upper curve is a Murnaghan fit of the (400) reflection experimental data for the cubic phase. The data for (222), (440), and (622) reflections are also shown. Lower curve is a Murnaghan fit of V/V_0 derived from 10 lattice spacings of the monoclinic B phase.

TABLE II. Observed and calculated lattice spacings d_{hkl} of monoclinic Yb_2O_3 at zero pressure, after pressure release, using the lattice parameters determined by Hoekstra (Ref. 17).

$h\,k\,l$	d_{obs} (Å)	d_{calc} (Å)
2 0 2	3.286	3.292
1 1 1	3.015	3.038
4 0 1	2.952	2.954
4 0 $\bar{2}$	2.890	2.883
0 0 3	2.785	2.773
3 1 0	2.735	2.726
1 1 $\bar{2}$	2.698	2.651
6 0 0	2.232	2.252
5 1 $\bar{1}$	2.129	2.128
3 1 $\bar{3}$	2.057	2.057
3 1 3	1.857	1.848
8 0 $\bar{1}$	1.721	1.716
7 1 $\bar{2}$	1.649	1.650
7 1 1	1.603	1.601
8 0 2	1.478	1.477

$$V/V_0=[1+P(B_0'/B_0)]^{-1/B_0'},$$

where B_0 is the isothermal bulk modulus and B_0' its pressure derivative at ambient pressure and temperature. V_0 was allowed to vary, as the zero pressure a value may be submitted to some uncertainty. The calculated curve (Fig. 5) represents the Murnaghan equation of state obtained from the fit of the (400) reflection. The selected set of B_0, B_0', and V_0 values are

$$B_0=181(1)\text{ GPa},\quad B_0'=7.3(2),$$

and

$$V_0=1133.5(3)\text{ Å}^3.$$

Taking advantage that the high-pressure B phase is retained after releasing the pressure, a detailed analysis of this phase was performed at atmospheric pressure using a different diffraction angle in order to get a better resolution. This allowed us to deconvoluate most of the overlapping peaks. The results of this analysis are presented in Table II, where the d_{hkl} values are compared with those calculated using the lattice parameters determined by Hoekstra (see above). The agreement is rather good. The initial lattice volume of the B-phase is noted V_0' as the zero (ambient) pressure reference: $V_0'=391(1)$ Å^3.

On the other hand, the fit of the 15 lattice plane spacings d_{hkl} given in Table II leads to the following parameters:

$$a=13.707(7)\text{ Å},\quad b=3.432(1)\text{ Å},\quad c=8.504(3)\text{ Å},$$

$$\beta=100.526(3)^\circ,\quad\text{and}\quad V_0'=393.3(4)\text{ Å}^3.$$

Similar fits have been done for d spacings of the B phase at 15.5, 18.5, 20.7, and 25 GPa, taking into account only the best defined peaks among the 15 selected at zero pressure, i.e., 10, 12, 11, and 8 peaks, respectively. The corresponding lattice parameters as well as the relative volume V/V_0' are given in Table III. Note that V_0' refers to six molecules per unit cell. A fit to the Murnaghan equation of state has been performed for the B phase too, however with less accuracy, considering that only the ambient pressure data are available in the low-pressure range. Furthermore there is some correlation between the values of B_0 and B_0', a smaller B_0' value giving a larger B_0 value and vice versa. The most probable solutions may be those involving B_0 values higher or equal to the one found for the cubic phase, thus leading to small B_0'. The fit displayed in Fig. 5 was obtained after normalization of the molecular volume for the two phases and assuming equal B_0 for the two structures. It corresponds to

$$B_0=181\text{ GPa},\quad B_0'=1.3,\quad\text{and}\quad V_0=1043\text{ Å}^3.$$

The calculated values of V/V_0 according to these laws are reported in Table I for the two phases. Note that the volume jump is 8% at the structural phase transition.

VI. DISCUSSION

Structural phase transition

The *in situ* high-pressure measurements performed at room temperature with EDXRD and those at 4.2 K with ^{170}Yb Mössbauer spectroscopy agree quite well. Both sets of data provide clear evidence for a structural transformation from a cubic C-type phase to a monoclinic B-type phase when applying pressure above about 13 GPa. Furthermore they show that the high-pressure B phase is retained after releasing the pressure, as expected for a reconstructive phase transition. It should be emphasized that the transition pressure we found (13 GPa) is significantly higher than those known (2.5–3.5 GPa) from static high-pressure experiments which were, however, carried out at high temperatures (550–1450 °C).[17] Nevertheless the C-B phase boundary in Yb_2O_3 is expected to occur at about 5 GPa by extrapolating the high-temperature Hoekstra data to room-temperature. This suggests, following Atou *et al.*[9] that the pressure-induced C to B transition, observed in Yb_2O_3, proceeds via the A phase. It is worth noticing that Fujimura *et al.*[10] report-

TABLE III. Pressure variation of the lattice constants of monoclinic Yb_2O_3 derived from the high-pressure x-ray diagrams. V_0' was derived from the zero-pressure diagram ($V_0'=393.3$ Å^3). V/V_0 refers to the cubic lattice unit cell volume and corresponds to experimental data of Fig. 5.

P (GPa)	a (Å)	b (Å)	c (Å)	β (deg)	V/V_0'	V/V_0
15.5	13.26(2)	3.41(2)	8.13(4)	98.6(2)	0.92(1)	0.853(8)
18.5	13.15(1)	3.380(1)	8.126(2)	98.67(3)	0.908(2)	0.838(1)
20.7	13.04(4)	3.395(5)	8.10(3)	98.0(3)	0.903(8)	0.833(7)
25.0	12.91(7)	3.364(7)	8.02(3)	97.3(2)	0.88(1)	0.81(1)

TABLE IV. ^{170}Yb zero-pressure lattice quadrupole splitting parameters in Yb_2O_3 (cubic phase) calculated in a point-charge model approximation (PCM). Comparison with values derived from ^{155}Gd Mössbauer data in Gd_2O_3 and ^{111}Cd PAC results in Yb_2O_3 using: $Q_{Yb}=-2.14b\,(1-\gamma_\infty)_{Yb}=81$ and $(1-\gamma_\infty)_{Gd}Q_{Gd}=121$b. The lattice parameters of the C-type Gd_2O_3 and Yb_2O_3 were taken to be 10.8122 and 10.4342 Å, respectively.

	Δ_l (C_{3i}) (mm/s)	Δ_l (C_2) (mm/s)	η_l (C_2)
PCM	−16.99	7.78	0.51
^{155}Gd	−17.11	8.41	0.66
^{111}Cd	−14.40	9.07	0.75

ed in their room-temperature high-pressure x-ray-diffraction experiments a C to A phase transition occurring at 15 GPa in Yb_2O_3. Thus it seems that slightly different experimental conditions tend to favor either the B or the A phase. The $B\rightarrow A$ or $A\rightarrow B$ transition requires little energy because it is a displacive-type transformation (the B phase is a slight deformation of the A phase). This is further demonstrated by extensive shock compression or static pressure experiments on rare earth sesquioxides which showed C-type$\rightarrow A$-type transition during loading and A-type$\rightarrow B$-type transformation on unloading.[9]

Volume dependence of the hyperfine interaction parameters

In the following, we try to evaluate the correlation between the volume contraction with pressure and the variation of the hyperfine data derived from Mössbauer spectra, namely the quadrupole splitting. The isomer shift ($\cong 0.1$ mm/s) is in our case ($0\rightarrow 2$ transition) irrelevant because it is smaller than the Mössbauer linewidth ($\Gamma_0\cong 2$ mm/s).[27]

The electric field gradient (EFG) tensor V_{ij}, which interacts with the nuclear quadrupole moment Q of the ytterbium nucleus, leads to the so-called electrostatic quadrupole interaction, which is commonly characterized by $\Delta=eQV_{zz}$ and η. The EFG has two significant sources.[28] The first of these arises from the asymmetry of the lattice charge distribution (V_{ij}^l) and the second is provided by the nonspherical $4f$ valence shell (V_{ij}^v):

$$V_{ij}=(1-\gamma_\infty)V_{ij}^l+(1-R_Q)V_{ij}^v\ , \qquad (1)$$

where γ_∞ is the Sternheimer antishielding factor, and R_Q a shielding factor to account for the polarization of the initially symmetric core orbitals. Equation (1) assumes that the systems of principal axes coincide as is normally the case.

The lattice contribution is generally estimated using a point-charge model summation over the lattice. The determination of the pressure dependence of the lattice parameters as deduced from our EDXRD data allows us to extract the Δ_l vs P relationship, assuming no change in the atomic positions. Hence the volume dependence of the $4f$ contribution Δ_v to the quadrupole interaction can be evaluated. This latter contribution is of special interest because it is related to the electronic structure of the Yb^{3+} ions in the lattice (Δ_v and η_v are thermal average over the wave functions of the crystal-field levels).

We made several attempts to evaluate the lattice contribution Δ_l at ^{170}Yb in Yb_2O_3, using successively a point-charge model (PCM), ^{155}Gd Mössbauer quadrupole interaction data in the isostructural Gd_2O_3 compound,[29,30] and finally, ^{111}Cd perturbed angular correlation (PAC) data for Yb_2O_3 and the whole R_2O_3 series.[12–14] These evaluations for the cubic C phase are compared in Table IV.

In the following we will restrict our discussion to the behavior of the C phase only. In order to estimate the pressure (volume) dependence of Δ_l it is tempting to assume that it should scale linearly with a^{-3}, where a is the lattice parameter at a given pressure. However ^{111}Cd PAC data for the C-R_2O_3 series (including In_2O_3 and Sc_2O_3 with smaller a parameter than the rare-earth sesquioxides) evidence more complex behaviors. Shitu *et al.*[12] found a nearly linear dependence of $\Delta_l(C_2)$ with a^{-3} and a nearly constant value of $\Delta_l(C_{3i})$. On the other hand, $\eta(C_{3i})=0$ for the whole series and $\eta(C_2)$ increases with the lattice constant. These behaviors were attributed to changes of the position of the atoms in the unit cell in the different R_2O_3 compounds.[13] Thus the pressure (volume) dependence of Δ_l in C-Yb_2O_3 was estimated from the PAC data (Fig. 8 of Ref. 12) assuming that the pressure effect is equivalent to a decrease of the size of the R atoms in the R_2O_3 series. The results of this analysis, which allow us to evaluate the volume dependence of the valence contributions to Δ and η, are reported in Table V. The main effect of the pressure is to decrease Δ_v for the C_2 site. Notice that Δ_v values are considerably smaller than the free ion ($|J_z\rangle=|\pm 7/2\rangle$) value of about 46.4 mm/s, as expected for a crystal-field ground state of predominant $|J_z\rangle=|\pm 1/2\rangle$ character. The leading term, B_2^0, of the crystal-field Hamiltonian is positive

TABLE V. Pressure dependence of the lattice quadrupole splitting in cubic Yb_2O_3 derived from ^{111}Cd PAC results in the R_2O_3 series. Computed corresponding valence contribution. Notice that the negative η values indicate an interchange of the x and y EFG axes.

P (GPa)	V/V_0	a^{-3} (10^{-4} Å^{-3})	Δ_l (C_{3i}) (mm/s)	Δ_l (C_2) (mm/s)	η_l (C_2)	Δ_v (C_{3i}) (mm/s)	Δ_v (C_2) (mm/s)	η_v (C_2)
0	1	8.8(1)	−14.4(2)	9.0(2)	0.75(2)	25.5(5)	16.1(3)	−0.26(9)
4.2	0.977	9.0(1)	−14.3(2)	9.6(2)	0.75(2)	25.3(6)	14.2(4)	−0.09(8)
12	0.945	9.3(1)	−14.5(2)	10.3(2)	0.73(2)	24.7(8)	12.7(4)	−0.1(1)
13.6	0.940	9.4(1)	−14.5(2)	10.5(2)	0.72(2)	24.5(9)	12.5(4)	0.1(1)

for the C_2 site and increases with pressure as shown by the volume dependence of $\Delta_l(C_2)$.

VII. CONCLUSION

In this work we have reported a very-high-pressure Mössbauer study with the high transition energy ^{170}Yb isotope, using a diamond anvil cell. We demonstrated that the use of DAC is not restricted to low energy (<30 keV) Mössbauer isotopes when special care is taken for the collimation of gamma rays.[31,32] The accuracy of the hyperfine parameters of Yb_2O_3 measured under these conditions is quite satisfactory and the Mössbauer results can be compared with the structural data in a coherent way.

The occurrence of a pressure-induced structural transition from cubic (C) to monoclinic (B) Yb_2O_3 has also been observed at room temperature. Application of a pressure of about 13 GPa is sufficient to complete the $C \rightarrow B$ transformation. The transition is of reconstructive type, the monoclinic phase is retained after releasing the pressure. The pressure (volume) dependence of the lattice EFG for the C-type Yb_2O_3 phase was estimated from PAC data for the rare-earth sesquioxide series. This allowed us to evaluate the $4f$ contribution to the EFG and its volume dependence.

Finally we want to emphasize that high pressure ^{170}Yb Mössbauer spectroscopy is a unique tool for the study of ytterbium-based heavy fermion materials of current interest today.[33] This technique is unique in the sense that it is so far the only method well suited to study their magnetic properties at pressure above 10 GPa. Furthermore the small size of the pressure cell is well suited for measurements below 4.2 K or even 1.5 K often required for the studies of heavy fermion or Kondo systems.

ACKNOWLEDGMENTS

It is a pleasure to acknowledge M. Pasternak and G. Hearne for enlightening advice and discussions. We also thank Cl. Jeandey, C. Ayache, J. Hodges, and P. Bonville for helpful discussions and L. Trabut for technical assistance.

*On leave from Laboratoire de Spectrométrie Physique, Université Joseph-Fourier, Grenoble 1, France. Present address: Laboratoire de Magnétisme Louis-Néel, CNRS BP 166, 38042 Grenoble Cedex 9, France.

[1]R. D. Taylor, M. P. Pasternak, and R. Jeanloz, J. Appl. Phys. **69**, 6126 (1991).
[2]M. P. Pasternak, R. D. Taylor, A. Chen, C. Meade, L. M. Falicov, A. Giesekus, R. Jeanloz, and P. Y. Yu, Phys. Rev. Lett. **65**, 790 (1990).
[3]A. Gleissner, W. Potzel, J. Moser, and G. M. Kalvius, Phys. Rev. Lett. **70**, 2032 (1993).
[4]M. P. Pasternak, R. D. Taylor, M. B. Kruger, R. Jeanloz, J. P. Itié, and A. Polian, Phys. Rev. Lett. **72**, 2733 (1994).
[5]E. Sterer, M. P. Pasternak, and R. D. Taylor, Rev. Sci. Instrum. **61**, 1117 (1990).
[6]M. P. Pasternak and R. D. Taylor, Hyperfine Interact. **62**, 89 (1990).
[7]M. Schöppner, J. Moser, A. Kratzer, U. Potzel, J. M. Mignot, and G. M. Kalvius, Z. Phys. B **63**, 25 (1986).
[8]J. Moser, K. H. Münch, and G. M. Kalvius, Hyperfine Interact. **40**, 405 (1988).
[9]T. Atou, K. Kusaba, K. Fukuoka, M. Kikuchi, and Y. Syono, J. Solid State Chem. **89**, 378 (1990). See also Y. Syono, High Pressure Res. (to be published).
[10]A. Fujimura, T. Kikegawa, and H. Iwasaki, unpublished results mentioned in Ref. 9.
[11]G. Chen, J. R. Peterson, and K. E. Brister, J. Solid State Chem. **111**, 437 (1994).
[12]J. Shitu, D. Wiarda, T. Wenzel, M. Uhrmacher, K. P. Lieb, S. Bedi, and A. Bartos, Phys. Rev. B **46**, 7987 (1992).
[13]A. Bartos, D. Wiarda, M. Uhrmacher, and K. P. Lieb, Hyperfine Interact. **80**, 953 (1993).
[14]D. Wiarda, M. Uhrmacher, A. Bartos, and K. P. Lieb, J. Phys. Condens. Matter **5**, 4111 (1993).
[15]A. F. Pasquevich, A. G. Bibiloni, C. P. Mossolo, M. Rentería, J. A. Vercesi, and K. Freitag, Phys. Rev. B **49**, 14 331 (1994).
[16]L. Eyring, in *Handbook on the Physics and Chemistry of the Rare Earths,* edited by K. A. Gschneidner and L. Eyring (North-Holland, Amsterdam, 1979), Vol. 3, p. 339.
[17]H. R. Hoekstra, Inorg. Chem. **5**, 754 (1966).
[18]J. P. Coutures, J. Coutures, R. Renard, and G. Benezech, C. R. Acad. Sci. **275**, 1203 (1972).
[19]T. Schleid and G. Meyer, J. Less-Common Met. **149**, 73 (1989).
[20]E. Schweda, Key Eng. Mat. **68**, 187 (1992).
[21]F. Gonzalez-Jimenez, P. Imbert, J. C. Achard, and A. Percheron, Phys. Status Solidi A **19**, 201 (1973).
[22]R. Le Toullec, J. P. Pinceaux, and P. Loubeyre, High Pressure Res. **1**, 77 (1988).
[23]H. Bonrath, K. H. Hellwege, K. Nicolay, and G. Weber, Phys. Kondens. Mater. **4**, 382 (1966).
[24]R. M. Moon, W. C. Koehler, H. R. Child, and L. J. Raubenheimer, Phys. Rev. **176**, 722 (1968).
[25]G. M. Kalvius, G. K. Shenoy, and B. D. Dunlap, *Colloques Internationaux du CNRS* (CNRS, Paris, 1970), Vol. 180 II, p. 477.
[26]I. Nowik and E. R. Bauminger, in *Mössbauer Effect Data Index 1975,* edited by J. G. Stevens and V. E. Stevens (Plenum, New York, 1976), p. 407.
[27]P. Bonville, P. Imbert, G. Jehanno, and F. Gonzalez-Jimenez, J. Phys. Chem. Solids **39**, 1273 (1978).
[28]R. G. Barnes, R. L. Mössbauer, E. Kankeleit, and J. M. Poindexter, Phys. Rev. **136**, A175 (1964).
[29]J. D. Cashion, D. B. Prowse, and A. Vas, J. Phys. C **6**, 2611 (1973).
[30]W. A. Barton and J. D. Cashion, J. Phys. C **12**, 2897 (1979).
[31]F. M. Mulder and R. C. Thiel, Rev. Sci. Instrum. **65**, 707 (1994).
[32]F. M. Mulder and R. C. Thiel, Europhys. Lett. **25**, 657 (1994).
[33]Z. Fisk and M. B. Maple, J. Alloys Comp. **183**, 303 (1992).